

# Theory of magnetic excitations in iron-based layered superconductors

M.M. Korshunov<sup>1,2\*</sup> and I. Eremin<sup>1,3</sup>

<sup>1</sup>*Max-Planck-Institut für Physik komplexer Systeme, D-01187 Dresden, Germany*

<sup>2</sup>*L.V. Kirensky Institute of Physics, Siberian Branch of Russian Academy of Sciences, 660036 Krasnoyarsk, Russia and*

<sup>3</sup>*Institute für Mathematische und Theoretische Physik,  
TU Braunschweig, D-38106 Braunschweig, Germany*

(Dated: April 10, 2008)

Based on the effective four-band model we analyze the spin response in the normal and superconducting states of the Fe-pnictide superconductors. While the normal state spin excitations are dominated by the continuum of the interorbital antiferromagnetic fluctuations and the intraband spin density wave fluctuations, the unconventional superconductivity yields different feedback. The resonance peak in form of the well-defined spin exciton occurs *only* for the interband scattering at the antiferromagnetic momentum  $\mathbf{Q}_{AFM}$  for the  $s_{\pm}$  (extended  $s$ -wave) superconducting order parameter and it disappears rapidly for  $\mathbf{q} < \mathbf{Q}_{AFM}$ . The resonance feature is extremely weak for the  $d_{x^2-y^2}$ -wave order parameter due to specific Fermi surface topology of these compounds. The essential difference between  $s_{\pm}$ -wave and  $d_{x^2-y^2}$ -wave symmetries for the magnetic excitations can be used for experimental determination of the superconducting wave function symmetry.

PACS numbers: 74.20.Mn, 74.20.Rp, 74.25.Ha, 74.25.Jb

The relation between unconventional superconductivity and magnetism is one of the most interesting topics in the condensed matter physics. In contrast to the usual electron-phonon mediated superconductors where the paramagnetic spin excitations are suppressed below superconducting transition temperature due to the formation of the Cooper pairs with total spin  $S = 0$ , in unconventional superconductors, such as layered cuprates or heavy fermion superconductors, a bound state (spin resonance) with a high intensity forms below  $T_c$ <sup>1,2,3</sup>. The fact that the superconducting gap is changing sign at a different parts of the Fermi surface together with a presence of the strong electronic correlations yields such an enhancement of the spin response<sup>4</sup>. Most interestingly, an observation of the resonance peak indicates not only that Cooper-pairing is unconventional but also that the magnetic fluctuations are most relevant for superconductivity<sup>5</sup>.

Since the discovery of superconductivity in the quaternary oxypnictides LaFePO<sup>6</sup> and LaNiPO<sup>7</sup>, a new class of high- $T_c$  materials with Fe-based layered structure is emerging<sup>8,9,10,11,12,13,14</sup>. Although the microscopic nature of superconductivity in these compounds remains unclear at present, certain aspects have been already discussed<sup>15,16,17,18,19,20,21,22,23,24,25,26,27</sup>. In particular, *ab initio* band structure calculations<sup>15,16,17,18,19,20</sup> have shown that the conductivity and superconductivity in these systems are associated with the Fe-pnictide layer, and the electronic density of states (DOS) near the Fermi level shows maximum contribution from the Fe-3*d* orbitals. The resulting Fermi surface consists of two hole (*h*) and two electron (*e*) pockets. The normal state magnetic spin susceptibility determined from these bands<sup>22</sup> exhibits both small  $\mathbf{q} \sim 0$  fluctuations and antiferromagnetic commensurate spin density wave (SDW) peaks.

In this Rapid Communication, using the four-band tight-binding model we study theoretically the spin re-

sponse in the normal and superconducting states of Fe-based pnictide superconductors. We show that the resulting magnetic fluctuation spectrum calculated within random-phase approximation (RPA) consists of two contributions. The first one is from the antiferromagnetic (AFM) spin fluctuations peaked at  $\mathbf{Q}_{AFM} = (\pi, \pi)$  arising due to the interband scattering. The second contribution comes from the intraband scattering and results in a broad continuum of the SDW fluctuations with a small momenta. We show that the unconventional superconductivity yields different feedback on the magnetic excitation spectrum. The resonance peak in form of the spin exciton occurs only for the interband scattering at the AFM momentum for the  $s_{\pm}$ -wave superconducting order parameter. This peak is confined to the AFM wave vector and disappears rapidly away from it. We suggest that the superconductivity is most likely  $s_{\pm}$ -wave and is driven by the repulsive interaction.

The Fe ions form a square lattice in the FeAs layer of LaFeAsO system, which is interlaced with the second square lattice of As ions. Due to the fact that As ions sit in the center of each square plaquette of the Fe lattice and are displaced above and below the Fe plane, the crystallographic unit cell contains two Fe and two As ions. The band structure calculations<sup>15,16,17,18,19,20</sup> show that three Fe-3*d* states ( $d_{xz}$ ,  $d_{yz}$ , and  $d_{xy}$ ) give the main contribution to the density of states close to the Fermi level and that these states disperse weakly in the  $z$ -direction. The resulting Fermi surface consists of two hole (*h*) pockets centered around the  $\Gamma = (0, 0)$  point and two electron (*e*) pockets centered around the  $M = (\pi, \pi)$  point of the *folded* Brillouin zone (BZ)<sup>18</sup>. Note, the *folded* BZ corresponds to the case of two Fe atoms per unit cell, and the wave vector  $(\pi, \pi)$  in the *folded* BZ corresponds to the  $(\pi, 0)$  wave vector in the *unfolded* BZ (related to the case of one Fe per unit cell). To model the resulting band structure we assume the following single-electron Hamil-

tonian

$$H_0 = - \sum_{\mathbf{k}, \alpha, \sigma} \epsilon^i n_{\mathbf{k}i\sigma} - \sum_{\mathbf{k}, i, \sigma} t_{\mathbf{k}}^i d_{\mathbf{k}i\sigma}^\dagger d_{\mathbf{k}i\sigma}, \quad (1)$$

where  $i = \alpha_1, \alpha_2, \beta_1, \beta_2$  refer to the band indices,  $\epsilon^i$  are the on-site single-electron energies,  $t_{\mathbf{k}}^{\alpha_1, \alpha_2} = t_1^{\alpha_1, \alpha_2} (\cos k_x + \cos k_y) + t_2^{\alpha_1, \alpha_2} \cos k_x \cos k_y$  is the electronic dispersion that yields hole pockets centered around the  $\Gamma$  point, and  $t_{\mathbf{k}}^{\beta_1, \beta_2} = t_1^{\beta_1, \beta_2} (\cos k_x + \cos k_y) + t_2^{\beta_1, \beta_2} \cos \frac{k_x}{2} \cos \frac{k_y}{2}$  is the dispersion that results in the electron pockets around the  $M$  point. Using the abbreviation ( $\epsilon^i, t_1^i, t_2^i$ ) we choose the parameters  $(-0.60, 0.30, 0.24)$  and  $(-0.40, 0.20, 0.24)$  for the  $\alpha_1$  and  $\alpha_2$  bands, respectively, and  $(1.70, 1.14, 0.74)$  and  $(1.70, 1.14, -0.64)$  for the  $\beta_1$  and  $\beta_2$  bands, correspondingly (all values are in eV).

In Figs. 1(a) and 2(a) we show the resulting band structure and the corresponding Fermi surface for the undoped case,  $x = 0$ . The Fermi surface consists of the two hole ( $\alpha_1$  and  $\alpha_2$ ) and two electron ( $\beta_1$  and  $\beta_2$ ) pockets. The  $\beta$  bands show much broader bandwidth and are degenerate along  $X - M$  direction which is a consequence of the hybridization of the underlying  $d_{xz}$  and  $d_{yz}$  orbitals within the *folded* BZ. The  $\alpha$  bands centered around the  $\Gamma$  point are narrower which also results in the significant contribution to the density of states. The chosen band structure reproduces correctly the local-density approximation (LDA) Fermi surface topology and the corresponding values of the Fermi velocities. In particular, we have selected the on-site energies and the hopping matrix elements assuming the compensated metal at zero doping and the filling factor  $n = 4$  (we further assume that there exists another band below the Fermi level which is fully occupied and not considered here). Additionally, we take into account the details of the electronic dispersions of the bands which form the corresponding hole and electron Fermi surface pockets. The comparison between our effective model and the *ab initio* density functional calculations<sup>15,16,17,18,20</sup> can be seen from Fig. 1(b) where we display the electronic dispersion from Ref. 15. Note, the hole Fermi surfaces shifted by  $(\pi, \pi)$  is fully nested with that of the electron pockets which is also in full agreement with LDA results. Here, the position of the chemical potential  $\mu$  has been deduced from the equation  $n = 4 + x$ . We note that although the Fermi surface obtained previously in the effective two-band model<sup>27</sup> reproduces correctly the one obtained within LDA calculations, the actual evolution of the dispersion deviates significantly.

Next we consider the one-loop contribution to the spin susceptibility that includes the intraband and the interband contributions:

$$\chi_0^{ij}(\mathbf{q}, i\omega_m) = -\frac{T}{2N} \sum_{\mathbf{k}, \omega_n} \text{Tr} [G^i(\mathbf{k} + \mathbf{q}, i\omega_n + i\omega_m) G^j(\mathbf{k}, i\omega_n) + F^i(\mathbf{k} + \mathbf{q}, i\omega_n + i\omega_m) F^j(\mathbf{k}, i\omega_n)]$$

where  $i, j$  again refer to the different band indices.  $G^i$

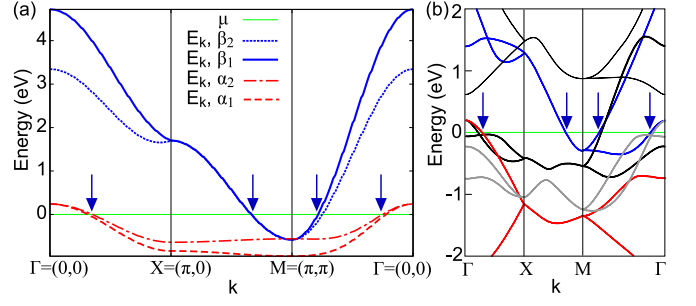


FIG. 1: (Color online) Calculated two-dimensional effective band structure along the main symmetry directions of the *folded* BZ (a) for the LaFeAsO system, and the reproduction (b) of the corresponding LDA band structure<sup>15,16,17,18,20</sup>. The arrows in (a) and (b) indicate the points where bands cross the Fermi level. Note, the shade (color) of the curves in (b) is used just as a guide to the eye and does not reflect the actual hybridization of the bands.

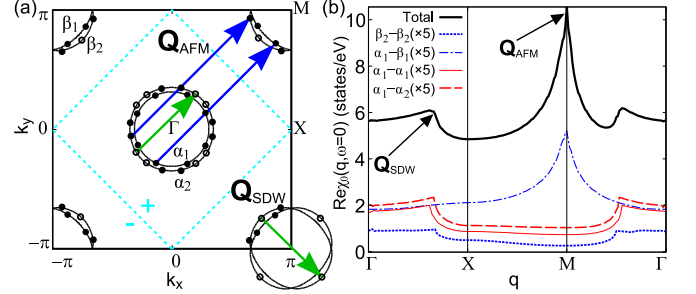


FIG. 2: (Color online) (a) Calculated Fermi surface topology for the LaFeAsO system. The arrows indicate the main scattering wave vectors. The filled dots refer to the states connected by the interband scattering at the AFM wave vector  $\mathbf{Q}_{AFM}$ , while the open dots denote the interband and intraband scattering at the incommensurate wave vector  $\mathbf{Q}_{SDW}$ . The dashed (cyan) lines and the  $+$ ,  $-$  signs depict the position of the nodes and the corresponding phase of the  $s_{\pm}$  superconducting order parameter. (b) Calculated real part of the one-loop spin susceptibility along the main symmetry directions of the first *folded* BZ. The thick solid (black) curve refer to the total susceptibility while the other (red and blue) curves refer to the partial contributions which are multiplied by a factor of 5 for the sake of the presentation. The main scattering wave vectors shown in (a) are also indicated in (b).

and  $F^i$  are the normal and anomalous (superconducting) Green functions, respectively.

In Fig. 2 we present the results for the real part of the total (physical) spin susceptibility  $\chi_0(\mathbf{q}, i\omega_m) = \sum_{i,j} \chi_0^{i,j}(\mathbf{q}, i\omega_m)$ , as well as the partial contributions. The total susceptibility is dominated by the scattering at the AFM wave vector  $\mathbf{Q}_{AFM}$  which is originated due to the interband ( $\alpha \rightarrow \beta$ ) scattering. It is interesting to note that the intraband and interband scattering within  $\alpha$  and  $\beta$  bands are very similar and are responsible for the broad hump around the  $\mathbf{Q}_{SDW}$  wave vector.

In the following we shall discuss the possible influence of the superconductivity driven by the short-range mag-

netic or charge fluctuations on the magnetic susceptibility. It has been already argued that most likely the superconductivity in these family of compounds is of unconventional origin and is driven either by the interband AFM fluctuations or by the intraband SDW fluctuations. However, one has to stress that even if the Cooper-pairing is driven by the interband fluctuations it still refers to the two fermionic states on the very same  $\alpha$  or  $\beta$  bands. The standard Cooper-pairing for the two fermions from the different bands will be suppressed, since there are no states with  $\mathbf{k}$  and  $-\mathbf{k}$  that can be connected at the different Fermi surfaces by the AFM momentum, as could easily be seen in Fig. 2(a). Therefore, we expect that inter-orbital AFM fluctuations will drive superconductivity in the  $\alpha$  and  $\beta$  bands. The latter should also result in the very same value of the superconducting gap in both bands. The repulsive nature of the interaction would then require<sup>28</sup> the superconducting gap that satisfies  $\Delta_{\mathbf{k}}^i = -\Delta_{\mathbf{k}+\mathbf{Q}_{AFM}}^j$ . Thus, we consider the magnetic susceptibility in the superconducting state assuming  $d_{x^2-y^2}$ -wave [ $\Delta_{\mathbf{k}} = \frac{\Delta_0}{2} (\cos k_x - \cos k_y)$ ] and  $s_{\pm}$ -wave [ $\Delta_{\mathbf{k}} = \frac{\Delta_0}{2} (\cos k_x + \cos k_y)$ ] symmetries of the order parameter which both satisfy the condition given above.

For the four-band model considered here the effective interaction will consist of the on-site Hubbard intraband repulsion  $U$  and the Hund's coupling  $J$ . There is also an interband Hubbard repulsion  $U'$ , which however does not contribute to the RPA susceptibility. Within RPA the spin response has a matrix form:

$$\hat{\chi}_{RPA}(\mathbf{q}, i\omega_m) = [\mathbf{I} - \mathbf{\Gamma}\hat{\chi}_0(\mathbf{q}, i\omega_m)]^{-1} \hat{\chi}_0(\mathbf{q}, i\omega_m) \quad (3)$$

where  $\mathbf{I}$  is a unit matrix and  $\hat{\chi}_0(\mathbf{q}, i\omega_m)$  is  $4 \times 4$  matrix formed by the interband and intraband bare susceptibilities determined by Eq. (2). The vertex is given by

$$\mathbf{\Gamma} = \begin{bmatrix} U & J/2 & J/2 & J/2 \\ J/2 & U & J/2 & J/2 \\ J/2 & J/2 & U & J/2 \\ J/2 & J/2 & J/2 & U \end{bmatrix}, \quad (4)$$

and we assume here  $J = 0.2U$  and  $U \sim t_1^{\beta_1}$ . Note that the value of  $U$  was chosen in order to stay in the paramagnetic phase. We have to note that our interaction parameters are carrying the band indices. Therefore, we neglect the possible orbital correlations. Whether this may play an important role needs to be addressed carefully and is beyond the scope of the present study. Though the current experimental and theoretical belief is such that the orbital physics is not involved in the physics of ferropnictides due to strong hybridization of all  $d$ -orbitals.

In Fig. 3(a) we show the results for the total RPA susceptibility,  $\chi_{RPA}(\mathbf{q}, i\omega_m) = \sum_{i,j} \hat{\chi}_{RPA}^{i,j}(\mathbf{q}, i\omega_m)$ , as a function of frequency at the AFM momentum  $\mathbf{Q}_{AFM}$ . One finds that in the normal state the spin response does not show a well-defined peak but rather a broad continuum of the spin fluctuations. The origin for this is that the RPA enhancement of the AFM spin fluctuations is determined by the  $\det[\mathbf{I} - \mathbf{\Gamma}\hat{\chi}(\mathbf{q}, i\omega_m)]$ . One

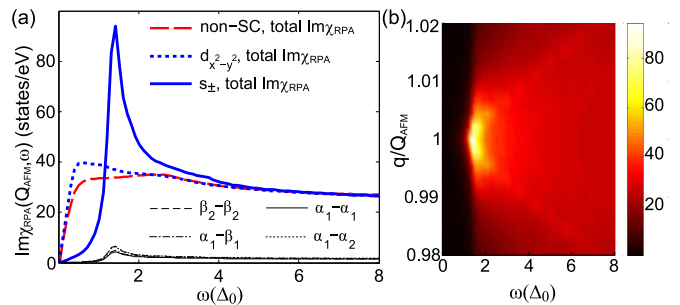


FIG. 3: (Color online) (a) Calculated imaginary part of the RPA spin susceptibility at the AFM wave vector  $\mathbf{Q}_{AFM}$  as a function of frequency in the normal and superconducting states. The thick dashed (red), dotted (blue), and solid (blue) curves correspond to the total RPA susceptibility. The thin (black) curves refer to the partial RPA contributions for the interband and intraband transitions in the  $s_{\pm}$  superconducting state. (b) Calculated imaginary part of the total RPA spin susceptibility in the  $s_{\pm}$  state as a function of frequency and momentum along (1,1) direction. For the numerical purposes we set the damping constant  $\delta^+ = 0.8$  meV.

has to remember that the intraband on-site Coulomb repulsion  $U$  will strengthen the corresponding intraband fluctuations and the Hund's exchange will only increase directly the instability towards interorbital AFM fluctuations. Given the fact that each of the bare susceptibilities slightly differ from band to band as shown in Fig. 2(b), the RPA does not yield a well-defined pole. Thus one obtains simply a continuum of the fluctuations. The situation changes in the superconducting state. The quasiparticles at the Fermi surface of the  $\alpha$  and  $\beta$  bands connected by the AFM wave vector possess the condition  $\Delta_{\mathbf{k}} = -\Delta_{\mathbf{k}+\mathbf{Q}_{AFM}}$  for the  $s_{\pm}$  order parameter. The imaginary part of the interband magnetic susceptibility is zero for small frequencies due to the opening of the gap, and then it experiences a discontinuous jump at  $\Omega_c = \min(|\Delta_{\mathbf{k}}| + |\Delta_{\mathbf{k}+\mathbf{Q}_{AFM}}|)$ . Correspondingly, the real part of the interband ( $\alpha \rightarrow \beta$ ) susceptibility will show the logarithmic singularity. This fulfils the resonance condition for the interband susceptibility:  $1 - (J/2)\text{Re}\chi_0^{\alpha\beta}(\mathbf{Q}_{AFM}, \omega_{res}) = 0$  and  $\text{Im}\chi_0^{\alpha\beta}(\mathbf{Q}_{AFM}, \omega_{res}) = 0$ . Moreover, the intraband bare susceptibilities are small at this wave vector due to the direct gap, *i.e.* no states at the Fermi level can be connected by the  $\mathbf{Q}_{AFM}$  for the intraband transitions. Therefore, a single resonant pole will occur for all components of the RPA spin susceptibility at  $\omega_{res} \leq \Omega_c$  and the spin excitation will form. This is evidently seen from Fig. 3(a). Due to the single pole in the denominator all components of the RPA susceptibilities behave very similarly and the total susceptibility shows a well-defined resonance peak.

In the case of  $d_{x^2-y^2}$  superconducting gap the situation is more complicated. As clearly seen from Fig. 2(a), the AFM wave vector connects states rather close to the node of the  $d_{x^2-y^2}$  superconducting order param-

ter and the overall gap in  $\text{Im}\chi_0^{\alpha\beta}$  determined by  $\Omega_c$  is small. At the same time even for this symmetry the resonance condition can be fulfilled due to the fact that  $\Delta_{\mathbf{k}} = -\Delta_{\mathbf{k}+\mathbf{Q}_{AFM}}$ . However, because of the smallness of  $\Omega_c \ll \Delta_0$  the total RPA susceptibility shows a moderate enhancement with respect to the normal state value, as seen in Fig. 3(a). Therefore, the resonance peak is pronounced only for the  $s_{\pm}$  order parameter. Such a distinct behavior for the two various order parameters can be clearly resolved by the inelastic neutron scattering experiments and therefore can be a direct tool to clarify the symmetry of the superconducting order parameter in these systems. Like for  $d_{x^2-y^2}$  case, we have also found that there is no spin resonance for  $d_{xy}$ - and  $d_{x^2-y^2} + id_{xy}$ -wave symmetries (due to their similarity we do not present these results).

Finally we address the evolution of the resonance peak away from the AFM wave vector. In Fig. 3(b) we show the total RPA susceptibility as a function of the momentum and frequency. Note that the  $s_{\pm}$  superconducting gap changes only slightly at the  $\alpha$  and  $\beta$  Fermi surfaces and can be considered nearly as a constant. Therefore, one always finds  $\Delta_{\mathbf{k}} = -\Delta_{\mathbf{k}+\mathbf{q}_n}$  as long as the wave vector  $\mathbf{q}_n < \mathbf{Q}_{AFM}$  connects the states at the Fermi surface of one of the  $\alpha$  and one of the  $\beta$  bands. However, as it is also clearly seen from Fig. 2(b) the nesting condition is very sensitive to the variation of  $\mathbf{q}_n$  away from  $\mathbf{Q}_{AFM}$ . Therefore, already at  $\mathbf{q}_n \approx 0.995\mathbf{Q}_{AFM}$  the

$\text{Re}\chi_0^{\alpha\beta}(\mathbf{q}_n, \omega_{res})$  is much smaller than its value at  $\mathbf{Q}_{AFM}$ . As a result the resonance peak is confined to the AFM momentum and does not disperse as it occurs for example in high- $T_c$  cuprates.

In conclusion, we have analyzed the behavior of the magnetic spin susceptibility in Fe-pnictide superconductors. We show that the magnetic fluctuation spectrum calculated within RPA consists of (i) the continuum of the AFM spin fluctuations peaked at  $\mathbf{Q}_{AFM} = (\pi, \pi)$  that arise due to the interband scattering, and (ii) a low- $\mathbf{q}$  fluctuations around the  $\mathbf{Q}_{SDW}$  due to the intraband scattering. We show that the unconventional superconductivity yields different feedback on the magnetic excitation spectrum. The resonance peak in form of the spin exciton occurs only for the interband scattering at the AFM momentum for the  $s_{\pm}$  superconducting order parameter. We also find that the resonance peak is confined to the AFM wave vector and disappears rapidly for  $\mathbf{q} < \mathbf{Q}_{AFM}$ .

*Note added.* After submission of our paper, we became aware of the experimental observation of the predicted resonance<sup>29</sup> and of the study by Meier and Scalapino<sup>30</sup> who reached some similar conclusions as ours.

We would like to thank A. Donkov, D. Parker, and P. Thalmeier for useful discussions. I.E. acknowledges support from Volkswagen Foundation.

\* Electronic address: maxim@mpipks-dresden.mpg.de

- <sup>1</sup> J. Rossat-Mignod, L.P. Regnault, C. Vettier, P. Bourges, P. Burllet, J. Bossy, J.Y. Henry, and G. Lapertot, *Physica C* **185-189**, 86 (1991).
- <sup>2</sup> N.K. Sato, N. Aso, K. Miyake, R. Shiina, P. Thalmeier, G. Varelogiannis, C. Geibel, F. Steglich, P. Fulde, and T. Komatsubara, *Nature* **410**, 340 (2001).
- <sup>3</sup> C. Stock, C. Broholm, J. Hudis, H.J. Kang, and C. Petrovic, *Phys. Rev. Lett.* **100**, 087001 (2008).
- <sup>4</sup> See, for example, M. Eschrig and M. R. Norman, *Phys. Rev. Lett.* **85**, 3261 (2000).
- <sup>5</sup> A. Abanov, A. Chubukov, and J. Schmalian, *Adv. Phys.* **52**, 119 (2003).
- <sup>6</sup> Y. Kamihara, H. Hiramatsu, M. Hirano, R. Kawamura, H. Yanagi, T. Kamiya, and H. Hosono, *J. Am. Chem. Soc.* **128**, 10012 (2006).
- <sup>7</sup> T. Watanabe, H. Yanagi, T. Kamiya, Y. Kamihara, H. Hiramatsu, M. Hirano, and H. Hosono, *Inorg. Chem.* **46**, 7719 (2007).
- <sup>8</sup> Y. Kamihara, T. Watanabe, M. Hirano, and H. Hosono, *J. Am. Chem. Soc.* **130**, 3296 (2008).
- <sup>9</sup> G.F. Chen, Z. Li, G. Li, J. Zhou, D. Wu, J. Dong, W.Z. Hu, P. Zheng, Z.J. Chen, H.Q. Yuan, J. Singleton, J.L. Luo, and N.L. Wang, *Phys. Rev. Lett.* **101**, 057007 (2008).
- <sup>10</sup> H. Yang, X. Zhu, L. Fang, G. Mu, and H.H. Wen, *Supercond. Sci. Technol.* **21**, 105001 (2008).
- <sup>11</sup> H.H. Wen, G. Mu, L. Fang, H. Yang, and X. Zhu, *Europhys. Lett.* **82**, 17009 (2008).
- <sup>12</sup> X.H. Chen, T. Wu, G. Wu, R.H. Liu, H. Chen, and D.F.

- Fang, *Nature* **453**, 761 (2008).
- <sup>13</sup> Z.A. Ren, J. Yang, W. Lu, W. Yi, G.C. Che, X.L. Dong, L.L. Sun, and Z.X. Zhao, *Europhys. Lett.* **82**, 57002 (2008); Z.A. Ren, J. Yang, W. Lu, W. Yi, G.C. Che, X.L. Dong, L.L. Sun, and Z.X. Zhao, *Mater. Research Innov.* **12**, in print (2008).
- <sup>14</sup> G.F. Chen, Z. Li, D. Wu, J. Dong, G. Li, W.Z. Hu, P. Zheng, J.L. Luo, N.L. Wang, *Chin. Phys. Lett.* **25**, 2235 (2008).
- <sup>15</sup> S. Lebegue, *Phys. Rev. B* **75**, 035110 (2007).
- <sup>16</sup> D.J. Singh and M.-H. Du, *Phys. Rev. Lett.* **100**, 237003 (2008).
- <sup>17</sup> L. Boeri, O.V. Dolgov, and A.A. Golubov, *Phys. Rev. Lett.* **101**, 026403 (2008).
- <sup>18</sup> I.I. Mazin, D.J. Singh, M.D. Johannes, and M.H. Du, *Phys. Rev. Lett.* **101**, 057003 (2008).
- <sup>19</sup> F. Ma and Z.-Y. Lu, *Phys. Rev. B* **78**, 033111 (2008).
- <sup>20</sup> K. Kuroki, S. Onari, R. Arita, H. Usui, Y. Tanaka, H. Kontani, and H. Aoki, *Phys. Rev. Lett.* **101**, 087004 (2008).
- <sup>21</sup> K. Haule, J.H. Shim, and G. Kotliar, *Phys. Rev. Lett.* **100**, 226402 (2008).
- <sup>22</sup> G. Xu, W. Ming, Y. Yao, X. Dai, S.-C. Zhang, and Z. Fang, *Europhys. Lett.* **82**, 67002 (2008).
- <sup>23</sup> J. Dong, H.J. Zhang, G. Xu, Z. Li, G. Li, W.Z. Hu, D. Wu, G.F. Chen, X. Dai, J.L. Luo, Z. Fang, and N.L. Wang, *Europhys. Lett.* **83**, 27006 (2008).
- <sup>24</sup> X. Dai, Z. Fang, Y. Zhou, and F.C. Zhang, *Phys. Rev. Lett.* **101**, 057008 (2008).
- <sup>25</sup> Q. Han, Y. Chen, and Z.D. Wang, *Europhys. Lett.* **82**

- 37007 (2008).
- <sup>26</sup> T. Li, J. Phys.: Condens. Matter **20**, 425203 (2008).
- <sup>27</sup> S. Raghu, X.-L. Qi, C.-X. Liu, D.J. Scalapino, and S.-C. Zhang, Phys. Rev. B **77**, 220503(R) (2008).
- <sup>28</sup> I. I. Mazin and V. M. Yakovenko, Phys. Rev. Lett. **75**, 4134 (1995).
- <sup>29</sup> A.D. Christianson, E.A. Goremychkin, R. Osborn, S. Rosenkranz, M.D. Lumsden, C.D. Malliakas, I.S. Todorov, H. Claus, D.Y. Chung, M.G. Kanatzidis, R.I. Bewley, and T. Guidi, arXiv:0807.3932 (unpublished).
- <sup>30</sup> T.A. Maier and D.J. Scalapino, Phys. Rev. B **78**, 020514(R) (2008).